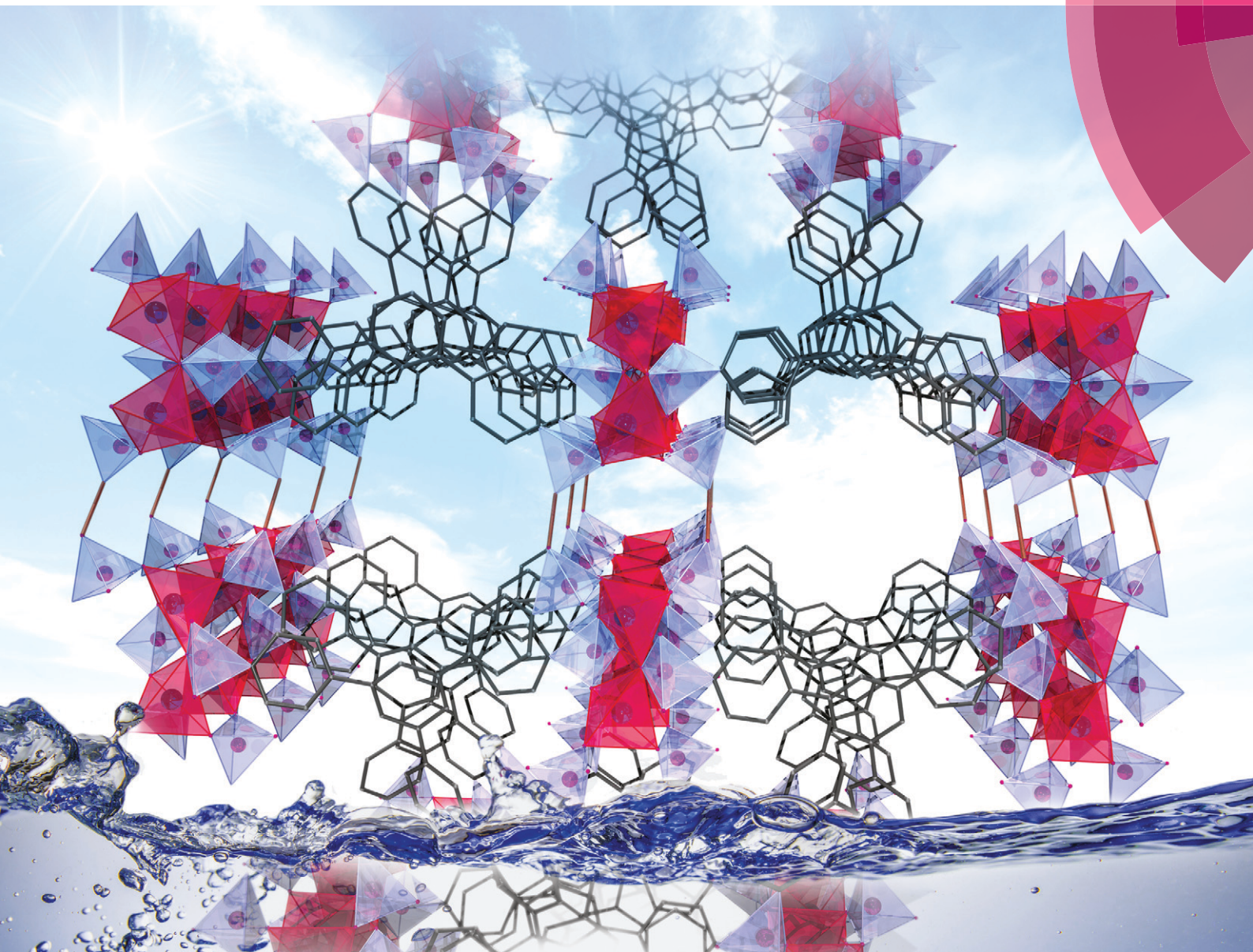


CrystEngComm

www.rsc.org/crystengcomm



COMMUNICATION

N. Stock *et al.*

Synthesis and characterisation of the porous zinc phosphonate
 $[\text{Zn}_2(\text{H}_2\text{PPB})(\text{H}_2\text{O})_2] \cdot x\text{H}_2\text{O}$

175 YEARS



Cite this: *CrystEngComm*, 2016, 18, 8147

Received 18th July 2016,
Accepted 8th August 2016

DOI: 10.1039/c6ce01580h

www.rsc.org/crystengcomm

Synthesis and characterisation of the porous zinc phosphonate $[\text{Zn}_2(\text{H}_2\text{PPB})(\text{H}_2\text{O})_2] \cdot x\text{H}_2\text{O}^\dagger$

N. Hermer,^a H. Reinsch,^a P. Mayer^b and N. Stock^{*a}

The synthesis, structure and properties of the new microporous zinc phosphonate $[\text{Zn}_2(\text{H}_2\text{PPB})(\text{H}_2\text{O})_2] \cdot x\text{H}_2\text{O}$ (denoted as CAU-25, CAU stands for Christian-Albrechts-University) are presented. The crystal structure was determined by combining single crystal and powder X-ray diffraction data. The final refinement was carried out by using the Rietveld method. The structure contains one-dimensional channels between dense, corrugated, hydrogen bonded layers with a diameter of approximately 5 Å. While N_2 uptake was not observed at 77 K, CO_2 and H_2O uptakes were measured at 298 K.

The intensely investigated field of metal–organic frameworks (MOF) offers materials with exceptional properties and remarkable structural versatility.¹ The possibility of tuning certain properties by isorecticular chemistry leads to a wide field of possible applications, for example in gas storage or separation, drug delivery, proton conductivity and catalysis.¹ The majority of MOFs are metal carboxylates; however, their stability towards moisture and temperature is often insufficient for applications under real life conditions. Due to the higher charge of phosphonate groups and the larger number of atoms involved in coordination to the metal ions, stronger metal–linker bonding is observed, which results in more stable compounds.² The various coordination modes and protonation states accessible to the phosphonate group also lead to large structural variability. A challenge in the synthesis of porous metal phosphonates is their tendency to form dense layered structures, and thus, the number of open framework metal phosphonates is very limited (Table S2a–d[†]).²

Different strategies have been used to prevent formation of the dense layered structures. For example, the use of methylphosphonic acid, which is too short to bridge the layers, led to porous compounds (Table S2a[†]).³ Other strategies are the insertion of another functional group (Table S2b[†]),⁴ which is coordinating to the metal, or using phosphonic acid monoester linkers, which could act like bidentate carboxylate-like groups (Table S2c[†]).⁵ A promising strategy is to disrupt the formation of a dense layered structure motif by adjustment of the geometry of the linker molecule (Table S2d[†]).^{6–9} The corresponding triphosphonic acids that have been successfully employed are listed in Fig. 1. 1,3,5-*tris*-(4-Phosphonophenyl)benzene (H_6PPB) has already been shown to lead to five metal phosphonates with a 3D framework structure (Table S3[†]),^{7–10} and three of them were successfully tested for porosity, $[\text{Sr}_2(\text{H}_2\text{PPB})(\text{CH}_3\text{OH})(\text{H}_2\text{O})_4]$,⁷ $[\text{Sn}(\text{H}_2\text{PPB})] \cdot 4.5\text{H}_2\text{O}$,⁸ and $[\text{Zr}(\text{H}_2\text{PPB})] \cdot 7\text{H}_2\text{O}$.⁹

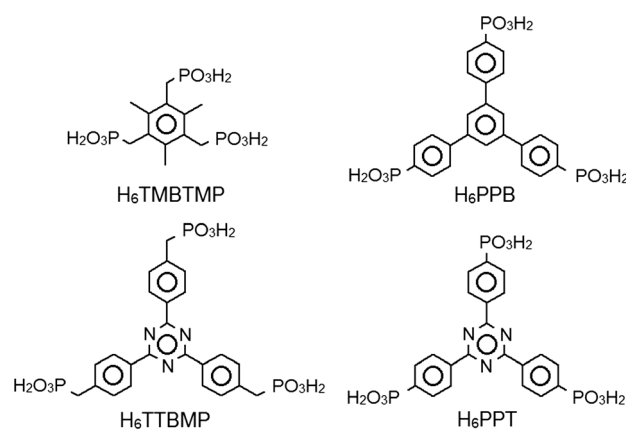


Fig. 1 Tritopic phosphonic acids that build 3D crystalline porous metal phosphonates (see also Table S2d[†]). H_6TMBTMP = (2,4,6-trimethylbenzene-1,3,5-triyl)tris(methylene)triphosphonic acid, H_6TTBMP = 2,4,6-*tris*[4-(phosphonomethyl)phenyl]-1,3,5-triazine, H_6PPB = 1,3,5-*tris*-(4-phosphonophenyl)benzene and H_6PPT = 2,4,6-*tris*-(phenylene-4-phosphonic acid)-s-triazine.

^a Christian-Albrechts-Universität, Max-Eyth-Straße 2, 24118 Kiel, Germany. E-mail: stock@ac.uni-kiel.de; Fax: +49 431 8801775; Tel: +49 431 8803261

^b Ludwig-Maximilians-Universität München, Department Chemie, Butenandtstr. 5-13, Haus F, 81377 München, Germany. E-mail: pemay@cup.uni-muenchen.de; Fax: +49 89 2180 77407; Tel: +49 89 2180 77399

[†] Electronic supplementary information (ESI) available. CCDC 1493141 contains the supplementary crystallographic data for CAU-25. For ESI and crystallographic data in CIF or other electronic format see DOI: 10.1039/c6ce01580h



Here, we report systematic studies of the system $\text{Zn}^{2+} : \text{H}_6\text{PPB} : \text{NaOH} : \text{H}_2\text{O} : \text{CH}_3\text{OH}$. The synthesis of the phosphonic acid H_6PPB was carried out in a three step reaction according to the literature,^{7,11} for which details can be found in the ESI.† First, 4-bromo-acetophenone was converted into *tris*(4-bromophenyl)benzene by cyclotrimerisation with thionylchloride.¹¹ By nickel(II) chloride catalysed cross-coupling of this compound with triethylphosphite, 1,3,5-*tris*(4-diethylphosphonophenyl)benzene was obtained.⁷ The hydrolysis of the diethylester to H_6PPB was subsequently carried out in concentrated HCl.⁷

High-throughput studies led to the new microporous zinc phosphonate $[\text{Zn}_2(\text{H}_2\text{PPB})(\text{H}_2\text{O})_2] \cdot x\text{H}_2\text{O}$, hereafter denoted as CAU-25 (CAU stands for Christian-Albrechts-University). The system $\text{Zn}^{2+} : \text{H}_6\text{PPB} : \text{NaOH} : \text{H}_2\text{O} : \text{CH}_3\text{OH}$ was studied using high-throughput methods,¹² which allow a fast and efficient investigation of different reaction parameters. Varying the molar ratios of $\text{Zn}^{2+} : \text{H}_6\text{PPB} : \text{NaOH}$ led to the title compound CAU-25 and two other crystalline products of low long range order (see Fig. S3 and S4†), which were not further characterized. Optimization of the molar ratios of the starting materials, the solvent mixture ($\text{H}_2\text{O} : \text{CH}_3\text{OH}$) as well as the synthesis temperature and time resulted in a highly crystalline product of CAU-25 (Table S4†). The optimized synthesis procedure is as follows: H_6PPB (30 mg, 55 mmol), aqueous 2 M $\text{Zn}(\text{NO}_3)_2$ (28 μL , 55 mmol), aqueous 2 M NaOH (55 μL , 110 mmol), 152 μL of deionised water and 366 μL of methanol were transferred to a Teflon-lined autoclave ($V_{\text{max}} = 2 \text{ mL}$) and sealed. The reactor was slowly heated to 120 °C within 24 h. The temperature was held for 24 h, and the reactor was subsequently cooled to room temperature within 16 h. The precipitate was filtered off and washed with water and methanol.

During synthesis optimisation, small single crystals (*ca.* 50 × 10 × 10 μm^3) of the title compound were obtained. Single-crystal X-ray diffraction (SC-XRD) data were recorded using a Nonius Kappa-CCD diffractometer at 173 K with monochromatic $\text{MoK}_{\alpha 1}$ radiation. However, due to the small size of the single crystals and the insufficient data quality, only a structure model could be determined. Thus, a combination of force-field calculations and Rietveld refinement was used to confirm and complete this model. In the first step, the approximate model obtained from SC-XRD was optimised using the universal force field as implemented in Materials Studio.¹³ The thus obtained model was subsequently refined by Rietveld methods using TOPAS.¹⁴ Additional electron density was observed in the difference Fourier map which was attributed to the presence of a non-coordinating water molecule. From thermogravimetric data and sorption measurements, the presence of a second water molecule is suggested, but it could not be assigned to electron density in the difference Fourier map, possibly as a result of disorder. Due to the large unit cell, the carbon backbone of the linker molecules was refined as a rigid body. The final Rietveld plot (Fig. 2), some relevant crystal data and the final figures of merit are provided in Table 1. Further details can be found in the ESI.†

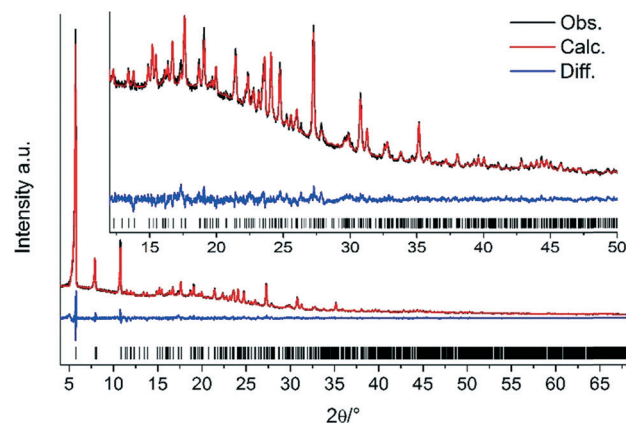


Fig. 2 The Rietveld plot for the refinement of CAU-25. The black line is the experimental data, the red line is the fit and the blue line is the difference curve. Vertical bars mark the Bragg reflection positions.

In the crystal structure of CAU-25, each Zn^{2+} ion exhibits a tetrahedral coordination environment consisting of four oxygen atoms of four different phosphonate groups. According to the Harris notation,¹⁵ the phosphonate groups exhibit [2.110] and [4.211] bonding modes. Corner-sharing of the ZnO_4 polyhedra leads to the formation of dimeric Zn_2O_7 units (Fig. 3a). These units are further connected *via* the phosphonate groups to form ribbons along the *c*-axis (Fig. 3b). Each ribbon is connected to four adjacent inorganic building units *via* the linker molecules (Fig. 3c) resulting in corrugated double layers of linker connected chains.

Based on $\text{O} \cdots \text{O}$ distances (Table S6†), possible hydrogen bonding can be anticipated which connects the double layers *via* $\text{P}-\text{O}-\text{H} \cdots \text{O}-\text{P}$ and $\text{P}-\text{O} \cdots \text{H}_2\text{O} \cdots \text{O}-\text{P}$ hydrogen bonds (Fig. 4 and S8†). The connection of adjacent corrugated double layers results in the formation of one-dimensional channels of approximately 5 Å in diameter along the *c*-axis (Fig. S9†) as determined using the van der Waals radii of the atoms lining the pore walls. The Connolly surface (Fig. 5) generated for a probe molecule with the kinetic diameter of CO_2 (3.3 Å) indicates kinetically inaccessible intralayer cavities and accessible interlayer channels. In contrast to other porous metal phosphonates, the structure of CAU-25 is a remarkable example due to the presence of interlayer porosity. Thermogravimetric measurements (Fig. 6 and Table S7†) showed a weight loss of 4% up to 100 °C and of 5% from 100 to 430 °C which is probably due to the loss of solvent

Table 1 Crystal data for CAU-25

Formula sum	$\text{Zn}_2\text{HO}_3\text{PC}_6\text{H}_4(\text{C}_6\text{H}_3)(\text{C}_6\text{H}_4\text{PO}_3)\text{C}_6\text{H}_4\text{PO}_3\text{H}$
Crystal system	Monoclinic
$a/\text{Å}, b/\text{Å}, c/\text{Å}$	44.673(4), 16.3110(8), 8.2967(3)
$\beta/^\circ$	95.301(8)
$V/\text{Å}^3$	6019.6(6)
Space group	$C2/c$
Atoms	39
λ	$\text{CuK}_{\alpha 1}$
$R_{\text{wp}}, R_{\text{Bragg}}$	3.45, 1.09
GoF	2.71



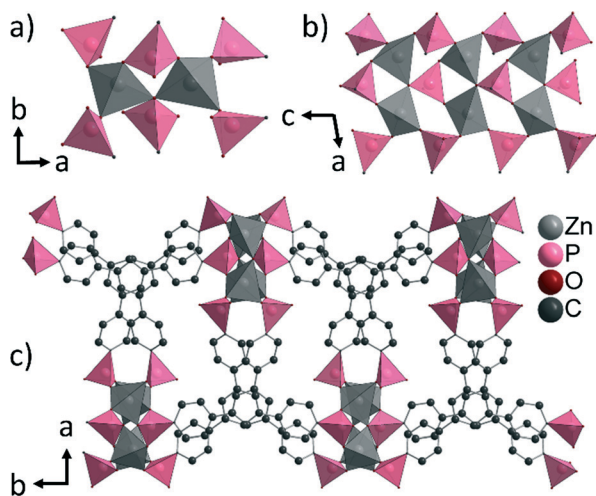


Fig. 3 Structure of CAU-25, a) dimeric Zn_2O_7 units with phosphonate groups (bonding modes [2.110] and [4.211]), b) ribbons of alternating corner-sharing Zn_2O_7 and O_3PC units, and c) a double layer formed through interconnection of the Zn-O-P ribbons by the linker molecules.

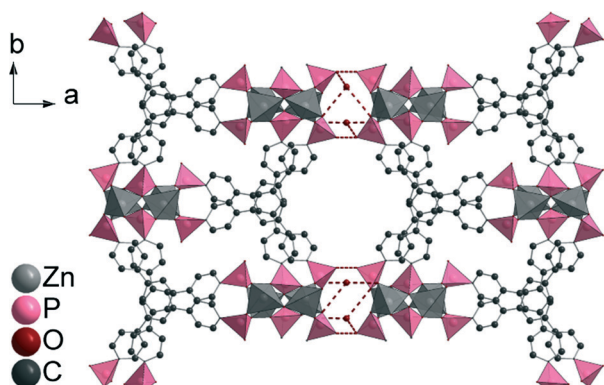


Fig. 4 Double layers of CAU-25, connected along the a -axis through hydrogen bonds (marked in red). Hydrogen bonds are postulated based on $\text{O}\cdots\text{O}$ distances.

molecules (calc. $-1.7\text{H}_2\text{O}$, 4%; $-2\text{H}_2\text{O}$, 5%). From 430 °C to 900 °C, the oxidation of the organic part occurs (obs. -41% ,

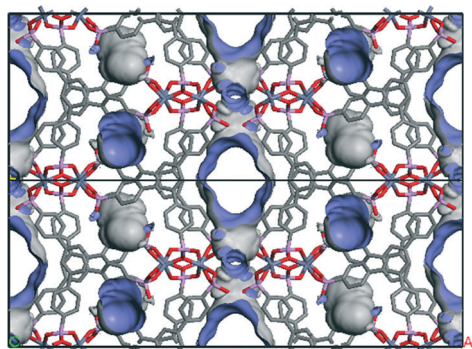


Fig. 5 Connolly surface of CAU-25 in a 1:2:1 supercell generated for a probe molecule with the kinetic diameter of CO_2 (3.3 Å). Kinetically inaccessible intralayer cavities and accessible interlayer channels are indicated. Protons are omitted for clarity.

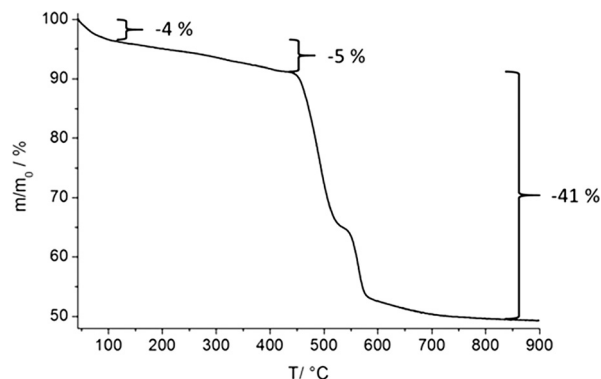


Fig. 6 Thermogravimetric measurement of CAU-25.

calc. -41%). Hence, CAU-25 was activated prior to sorption experiments at 150 °C for 18 h under reduced pressure (10^{-2} kPa). CAU-25 is not porous towards N_2 at 77 K (Fig. 7, right) but towards CO_2 (0.4 mmol g^{-1} (1.8 wt%) at 100 kPa) (Fig. 7, left) and water (7.3 mmol g^{-1} (13.2 wt%), Fig. 7, right) at 298 K, which is due to the dipole-dipole interactions of the latter two adsorptives with the framework and the higher measurement temperature that allows for higher framework flexibility and faster diffusion. The water vapour isotherm shows two steps. Initially, two water molecules per formula sum are adsorbed up to $p/p_0 = 0.35$, which corresponds to the two hydrogen bonded water molecules in between the double layers. At higher p/p_0 values, an uptake of three additional water molecules per formula sum is observed. In theory, the interlayer channels should be accessible for larger N_2 molecules. The reasons for this size selective porosity towards CO_2 is probably due to the higher temperature at which CO_2 sorption was measured. At lower temperatures, the mobility of gas molecules in narrow channels as in CAU-25 is often limited.⁷ The thermal stability of CAU-25 was evaluated by comparison of the PXRD patterns of the as-synthesized compound, the compound after activation and H_2O sorption measurements and the simulated PXRD pattern (Fig.

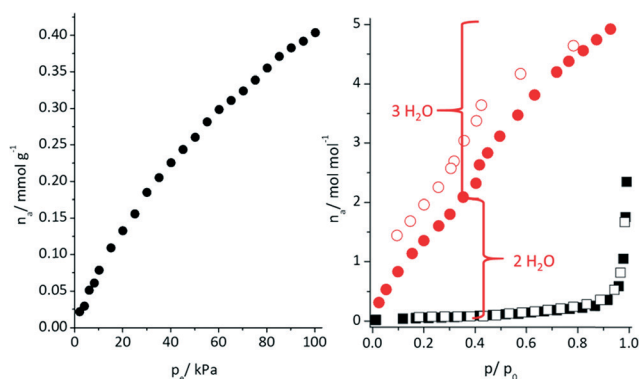


Fig. 7 Left: CO_2 sorption isotherm of CAU-25 (measured at 298 K); right: nitrogen (black symbols) and water sorption (red symbols) isotherms of CAU-25 (measured at 77 K and 298 K, respectively) (closed symbols, adsorption; open symbols, desorption), activation under vacuum (0.1 mbar).



S10†). While a decrease in long range order can be observed, the structure itself is retained.

Conclusions

The strategy to create porous metal phosphonates by disrupting the formation of a dense layered structure motif by adjustment of the geometry of the linker molecule seems to be very promising. Using this concept, we have been able to synthesize a new zinc phosphonate employing the triphosphonic acid 1,3,5-*tris*-(4-phosphonophenyl)benzene. The resulting compound $[\text{Zn}_2(\text{H}_2\text{PPB})(\text{H}_2\text{O})_2] \cdot x\text{H}_2\text{O}$ (CAU-25) crystallises in a layered structure, and hydrogen bonding between the layers leads to interlayer porosity. CAU-25 is permanently porous and thermally stable up to 400 °C. The structure determination was possible by a combination of single crystal X-ray diffraction, universal force-field calculations and Rietveld refinement. Although the compound is not porous towards N_2 , porosity was shown by CO_2 and H_2O sorption experiments.

Notes and references

- 1 Themed issue on Metal Organic Frameworks, *Chem. Rev.*, 2012, **112**, 673; Themed issue on Metal Organic Frameworks, *Chem. Soc. Rev.*, 2014, **43**, 5405.
- 2 A. Clearfield and K. Demandis, *Metal Phosphonate Chemistry: From Synthesis to Applications*, The Royal Society of Chemistry, Cambridge, UK, 2012; K. J. Gagnon, H. P. Perry and A. Clearfield, *Chem. Rev.*, 2012, **112**, 1034; G. K. H. Shimizu, R. Vaidhyanathan and J. M. Taylor, *Chem. Soc. Rev.*, 2009, **38**, 1430; K. Maeda, *Microporous Mesoporous Mater.*, 2004, **73**, 47; M. Taddei, F. Costantino and R. Vivani, *Eur. J. Inorg. Chem.*, 2016, DOI: 10.1002/ejic.201600207.
- 3 K. Maeda, Y. Kiyozumi and F. Mizukami, *Angew. Chem., Int. Ed. Engl.*, 1994, **33**, 2335; K. Maeda, J. Akimoto, Y. Kiyozumi and F. Mizukami, *Angew. Chem., Int. Ed. Engl.*, 1995, **34**, 1199.
- 4 J. A. Groves, S. R. Miller, S. J. Warrender, C. Mellot-Draznieks, P. Lightfoot and P. A. Wright, *Chem. Commun.*, 2006, 3305; C. Serre, J. A. Groves, P. Lightfoot, A. M. Z. Slawin, P. A. Wright, N. Stock, T. Bein, M. Haouas, F. Taulelle and G. Férey, *Chem. Mater.*, 2006, **18**, 1451; Q. Yue, J. Yang, G.-H. Li, G.-D. Li and J.-S. Chen, *Inorg. Chem.*, 2006, **45**, 4431; M. T. Wharmby, S. R. Miller, J. A. Groves, I. Margiolaki, S. E. Ashbrook and P. A. Wright, *Dalton Trans.*, 2010, 39, 6389; M. T. Wharmby, J. P. S. Mowat, S. P. Thompson and P. A. Wright, *J. Am. Chem. Soc.*, 2011, **133**, 1266; M. T. Wharmby, G. M. Pearce, J. P. S. Mowat, J. M. Griffin, S. E. Ashbrook, P. A. Wright, L.-H. Schilling, A. Lieb, N. Stock, S. Chavan, S. Bordiga, E. Garcia, G. D. Pirngruber, M. Vreeke and L. Gora, *Microporous Mesoporous Mater.*, 2012, **157**, 3; S. Begum, Z. Wang, A. Donnadio, F. Costantino, M. Casciola, R. Valiullin, C. Chmelik, M. Bertmer, J. Kärger, J. Haase and H. Krautscheid, *Chem. – Eur. J.*, 2014, **20**, 8862; S. Begum, S. Horike, S. Kitagawa and H. Krautscheid, *Dalton Trans.*, 2015, 44, 18727.
- 5 S. S. Iremonger, J. Liang, R. Vaidhyanathan, I. Martens, G. K. H. Shimizu, T. D. Daff, M. Z. Aghaji, S. Yeganegi and T. K. Woo, *J. Am. Chem. Soc.*, 2011, **133**, 20048; S. S. Iremonger, J. Liang, R. Vaidhyanathan and G. K. H. Shimizu, *Chem. Commun.*, 2011, 47, 4430; J. M. Taylor, R. Vaidhyanathan, S. S. Iremonger and G. K. H. Shimizu, *J. Am. Chem. Soc.*, 2012, **134**, 14338.
- 6 J. M. Taylor, A. H. Mahmoudkhani and G. K. H. Shimizu, *Angew. Chem., Int. Ed.*, 2007, **46**, 795; N. Hermer and N. Stock, *Dalton Trans.*, 2015, 44, 3720; M. Taddei, F. Costantino, F. Marmottini, A. Comotti, P. Sozzani and R. Vivani, *Chem. Commun.*, 2014, **50**, 14831; S.-F. Tang, J.-J. Cai, L.-J. Li, X.-X. Lv, C. Wang and X.-B. Zhao, *Dalton Trans.*, 2014, 43, 5970.
- 7 R. Vaidhyanathan, A. H. Mahmoudkhani and G. K. H. Shimizu, *Can. J. Chem.*, 2009, **87**, 247.
- 8 R. K. Mah, M. W. Lui and G. K. H. Shimizu, *Inorg. Chem.*, 2013, **52**, 7311.
- 9 R. K. Mah, B. S. Gelfand, J. M. Taylor and G. K. H. Shimizu, *Inorg. Chem. Front.*, 2015, **2**, 273.
- 10 W. Ouellette, G. Wang, H. Liu, G. T. Yee, C. J. O'Connor and J. Zubietta, *Inorg. Chem.*, 2009, **48**, 953; M. Taddei, F. Costantino, R. Vivani, S. Sabatini, S.-H. Lim and S. M. Cohen, *Chem. Commun.*, 2014, **50**, 5737.
- 11 H. Zhi Guo, J. Liu, L. Gong An and D. Zhi Bing, *J. Chem. Res.*, 2003, **2003**, 778.
- 12 P. Maniam and N. Stock, in *Metal Phosphonate Chemistry: From Synthesis to Applications*, The Royal Society of Chemistry, 2012, p. 87; N. Stock, *Microporous Mesoporous Mater.*, 2010, **129**, 287–295.
- 13 *Materials Studio Version 5.0*, Accelrys Inc., San Diego, CA, 2009.
- 14 *Topas Academics 4.2*, Coelho Software, 2007.
- 15 R. A. Coxall, S. G. Harris, D. K. Henderson, S. Parsons, P. A. Tasker and R. E. P. Winpenny, *Dalton Trans.*, 2000, 2349.

